Acta Geodyn. Geomater., Vol. 21, No. 3 (215), 175–184, 2024
DOI: 10.13168/AGG.2024.0016
journal homepage: https://www.irsm.cas.cz/acta

ORIGINAL PAPER

QUANTITATIVE MICROSTRUCTURE CHARACTERIZATION FOR A RED-BED SOFT ROCK IN THE THREE GORGES RESERVOIR AREA

Guang LIU [1, 2, 3], Xudong GU [1], Fan YANG [1] *, Jun PENG [2, 3], Yun JIA [4] and Yiqiu FANG [1]

[1] *School of Civil Engineering, Hefei University of Technology, Hefei, Anhui 230009, China*
[2] *State Key Laboratory of Safety and Health for Metal Mines, Maanshan 243000, China*
[3] *Key Laboratory of Rock Mechanics and Geohazards of Zhejiang Province, Shaoxing, Zhejiang 312000, China*
[4] *University of Lille, CNRS, Centrale Lille, UMR9013, LaMcube, 59000 Lille, France*

**Corresponding author's e-mail:* fyang@hfut.edu.cn

ARTICLE INFO

Article history:
Received 27 May, 2024
Accepted 26 July 2024
Available online 2 September 2024

Keywords:
Damage constitutive model
Impact load
Frozen rock
Component combination
Weibull distribution

ABSTRACT

Red-bed soft rocks are commonly found in the bank slopes of reservoirs in southwestern China. The macroscopic mechanical behavior of red-bed soft rock is closely related to its microscopic particle structure. When studying the physical mechanism of landslide and collapse of red-bed soft rock slope, it is necessary to pay attention to the variation of its microstructure. Both CT scanning and optical microscope can observe the microscopic particle structure of the red-bed soft rock. However, quantitative analysis methods for these microscopic observation images are still rare. In this study, an optical microscope is used to observe a series of sections of the red-bed soft rock in the Three Gorges reservoir area. The image recognition method based on edge detection is adopted to extract the particle structure of the red-bed soft rock section from its microscopic image. A comparative analysis of various edge detection operators reveals that the Canny operator yields the most distinct particle contours with minimal distortion, effectively preserving the original morphology of particles and cement. Furthermore, a non-regular-shaped particle size representation is defined to statistically analyze the particle sizes of red-bed soft rocks. The heterogeneity index calculated using grain size difference was used to quantitatively evaluate the degree of heterogeneity in the microstructure of red-bed soft rock. Comparing the observed images and calculated rock particle data showed that this index accurately reflects the micro-geometric heterogeneity of the microstructure images. These findings provide a method for the quantitative analysis of the microstructure of red-bed soft rocks, offering valuable insights into their mechanical behavior.

1. INTRODUCTION

Red-bed soft rock is a unique type of rock frequently encountered in engineering projects in the southwestern region of China, and it is susceptible to softening and disintegration when interacting with water (Zhang et al., 2022). The mechanical properties of red-bed soft rocks directly affect the stability of engineering structures (Vlastelica et al., 2018; Knopp et al., 2022; Bilen et al., 2021). Many natural disasters, such as landslides and collapses, often occur in red-bed soft rock areas, causing huge economic and even life losses (Miščević et al., 2011; Miščević et al., 2020). With the development of the world economy and the need for infrastructure construction, the number and scale of projects in red-bed soft rock areas have been further increased. Because the mechanical properties of the rock mass can also be regarded as a reflection of its microstructure response to the load (Kazerani, 2013), the observation and analysis of microstructure are particularly prominent to better grasp the mechanical properties of red-bed soft rocks.

The Particle Flow Code (PFC) can be used to simulate the macroscopic mechanical properties of geotechnical materials on the basis of reproducing the microstructure of geotechnical materials. Especially with the proposal and wide application of the grain-based model (GBM) (Hofmann et al., 2015; Liu et al., 2018; Wang and Cai, 2018) researchers in rock mechanics are increasingly concerned with numerical modeling from the characteristics of rock microstructure. The GBM method approximates the real rock grain structure by combining regular balls or blocks to generate different shapes in the simulation. Certainly, the initial challenge of conducting such precise modeling lies in determining the details of the rock's grain structure, which necessitates the quantitative characterization of its microstructure.

Advancements in X-ray diffraction, scanning electron microscopy, computed tomography (CT), and other microscopic observation techniques have facilitated the study of the mechanics and deformation processes of rocks at the grain structure and mineral component level. This makes it possible to establish the relationship between the microstructural characteristics and the macroscopic mechanical properties. Zhao et al. (2022) employed Acoustic Emission (AE) surveillance

Cite this article as: Liu G, Gu X, Yang F, Peng J, Jia Y, Fang Y: Quantitative microstructure characterization for a red-bed soft rock in the Three Gorges Reservoir area. Acta Geodyn. Geomater., 21, No. 3 (215), 175–184, 2024**.** DOI: 10.13168/AGG.2024.0016

and computed tomography (CT) scanning to assess the progression of rock damage throughout the loading phase. Ding et al. (2003) measured the width of two CT-scale cracks in the rock at different stress stages by CT scanning the internal cracks of the rock.

Although various techniques, including CT scanning and optical microscopy, have been used to capture the microstructural features of rocks, quantitative analysis of these microscopic images remains a challenge (Goral et al., 2020). As pointed out by Zhao et al. (2023), CT scanning technology can reveal particle structures. However, this technology requires samples of specific sizes to achieve high-resolution imaging. Additionally, the analysis is easily influenced by subjective factors such as observer experience and fatigue. This makes it difficult to quantitatively analyze the microstructure of red-bed soft rocks. Consequently, despite advancements in imaging technology, extracting and quantitatively analyzing microstructural information from these images continues to be an active area of research.

Beyond merely extracting grain structures from microscopic images of red-bed soft rocks, it is equally important to conduct an accurate evaluation of these microstructures. Such an evaluation is essential for comprehending the microscopic traits of rocks. Multiple heterogeneity models including the uniform, Weibull, Gaussian, and Lorentz distribution models have been employed to investigate rock microstructure (Breithaupt et al., 2021; Wang et al., 2014; Zhao and Zhou, 2020). For instance, Liu et al. (2004) used the Weibull distribution model to characterize the heterogeneity of rocks and validated the model's accuracy through numerical simulation.

Therefore, this study investigates the quantitative analysis method of the microstructure of red-bed soft rocks in the Three Gorges Reservoir area in terms of both extraction and evaluation of the particle structure. Four edge detection algorithms were used to extract the grain structure from the microscopic images of red-bed soft rock, and the extraction accuracy of different edge detection algorithms was compared. The particle size of the red-bed soft rock was statistically analyzed. The heterogeneity index of the rocks was calculated based on the difference in particle size. The heterogeneity of the grain structure of the red-bed soft rock was quantitatively evaluated. The results can provide a theoretical basis for an in-depth understanding of the microscopic mechanisms of deformation and damage in red-bed soft rocks.

2. IMAGE RECOGNITION OF MICROSTRUCTURE

Extraction and recognition of rock microstructure is a complex task. Using image recognition to obtain rock grain structure features can save a great deal of time in manual processing. Several software and algorithms are available to extract fractures and pores (Li et al., 2018). However, there is a lack of research on the extraction of the complete grain structure. In this section, the grain structure under polarized light microscopy is converted into a binary image through a series of operations. The theory of edge detection is used to extract the edges of the grain structure.

2.1. SAMPLE PREPARATION

The sampling site was located at the Majiagou landslide in Pengjiapo Village, Zigui County, Hubei Province, within the Three Gorges reservoir area. Rock samples collected at the site were drilled with a rock coring machine. The two end faces of the rock samples were cut and smoothed with a rock cutting machine. The samples were then polished and processed into standard samples with a diameter of 50 mm and a height of 25 mm (Fig. 1).

Fig. 1 Red-bed soft rock samples.

To obtain a clear image of the microstructure, a representative flat section is taken from the surface of the sample for microstructure observation. Before microscopic observation, thin rock sections are first made (Fig. 2). The Leica DM750P polarizing microscope (Fig. 3) is used to observe the mineral grain structure and the cementation between minerals.

2.2. EDGE DETECTION METHOD FOR MICROSTRUCTURE

The edge of an image is one of its most basic features (Xie et al., 2020), representing the area where local brightness changes are most significant. The two most prominent aspects of this change are the rate of change and the direction, expressed by the gradient and direction, respectively (Cheng and Cui, 2008). The gradient is a vector, and its magnitude is measured by the amount of change per unit distance.Its direction is the one in which the equipotential surface changes the fastest. This direction is perpendicular to the equipotential surface.

Edge detection is essential to computer vision and image processing, providing vital information for subsequent work such as image recognition (Jing et al., 2022). The basic idea of edge detection, as the basis of the digital image processing process, is to emphasize the local edges in an image by utilizing edge enhancement operators. This algorithm defines

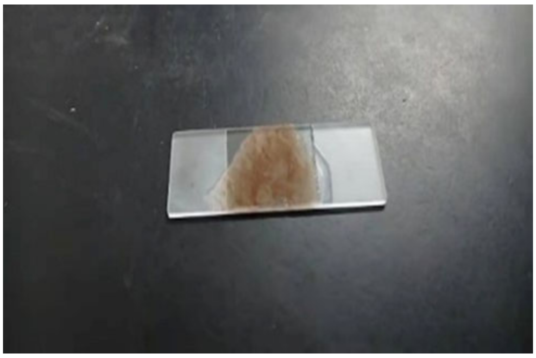

Fig. 2 Red-bed soft rock section.

Fig. 3 Polarized light microscope.

edge features based on pixel characteristics and identifies a set of edge points by applying a threshold. The boundary information of an image object can be used for image analysis, filtering, target recognition, and further image processing. Common edge detection operators include the Roberts, Sobel, Prewitt, and Canny operators.

(1) Roberts edge detection operator

The Roberts operator is an operator that uses a local difference operator to detect edges. This operator approximates the gradient magnitude to find edges by utilizing differences in intensity between diagonally adjacent pixels (Kang et al., 2008).

For quick and easy calculation of the gradient magnitude, an approximate formula can be used.

$$g(x,y)=\begin{Bmatrix}\left[\sqrt{f(x,y)}-\sqrt{f(x+1,y+1)}\right]^2+\\+\left[\sqrt{f(x+1,y)}-\sqrt{f(x,y+1)}\right]^2\end{Bmatrix}^{\frac{1}{2}} \tag{1}$$

(2) Sobel edge detection operator

The Sobel operator is mainly a weighting algorithm using the above and below, left and right neighbours of a pixel point. The algorithm used for the Sobel edge operator is a weighted average followed by a differentiation operation, which approximates the first-order derivative using differences (Li et al., 2012). The mathematical expression for this operation is as follows:

$$\begin{aligned}\Delta_x f(x,y)=&[f(x\text{-}1,y+1)+2f(x,y+1)+f(x+1,y+1)]\\&-[f(x\text{-}1,y\text{-}1)+2f(x,y\text{-}1)+f(x+1,y\text{-}1)]\end{aligned} \tag{2}$$

$$\begin{aligned}(\Delta_y f(x,y)=&[f(x\text{-}1,y\text{-}1)+2f(x\text{-}1,y)+f(x\text{-}1,y+1)]\\&-[f(x+1,y\text{-}1)+2f(x+1,y)+f(x+1,y+1)]\end{aligned} \tag{3}$$

(3) Prewitt edge detection operator

The Prewitt operator detects edges by using the principle that the grey level difference between the neighbouring points of a pixel reaches an extreme value at the edge. Prewitt combines local averaging and directional differencing by first averaging the filters and then applying directional differencing (Zhou et al., 2019). The mathematical expression for this operation is as follows:

$$\begin{aligned}\Delta_x f(x,y)=&[f(x+1,y+1)+f(x,y+1)+f(x-1,y+1)]\\&-[f(x+1,y-1)+f(x,y-1)+f(x-1,y-1)]\end{aligned} \tag{4}$$

$$\begin{aligned}\Delta_y f(x,y)=&[f(x-1,y-1)+f(x-1,y)+f(x-1,y+1)]\\&-[f(x+1,y-1)+f(x+1,y)+f(x+1,y+1)]\end{aligned} \tag{5}$$

(4) Canny edge detection operator

In 1986, John Canny pioneered the Canny edge detection algorithm, aiming for optimal detection by focusing on the best signal-to-noise ratio, localization accuracy, and one-sided response criteria (Canny, 1986). The specific implementation steps are as follows:

(I) Apply a Gaussian filter to smooth the image and reduce noise.

$$H(x,y)=exp(-\frac{x^2+y^2}{2\sigma^2}) \tag{6}$$

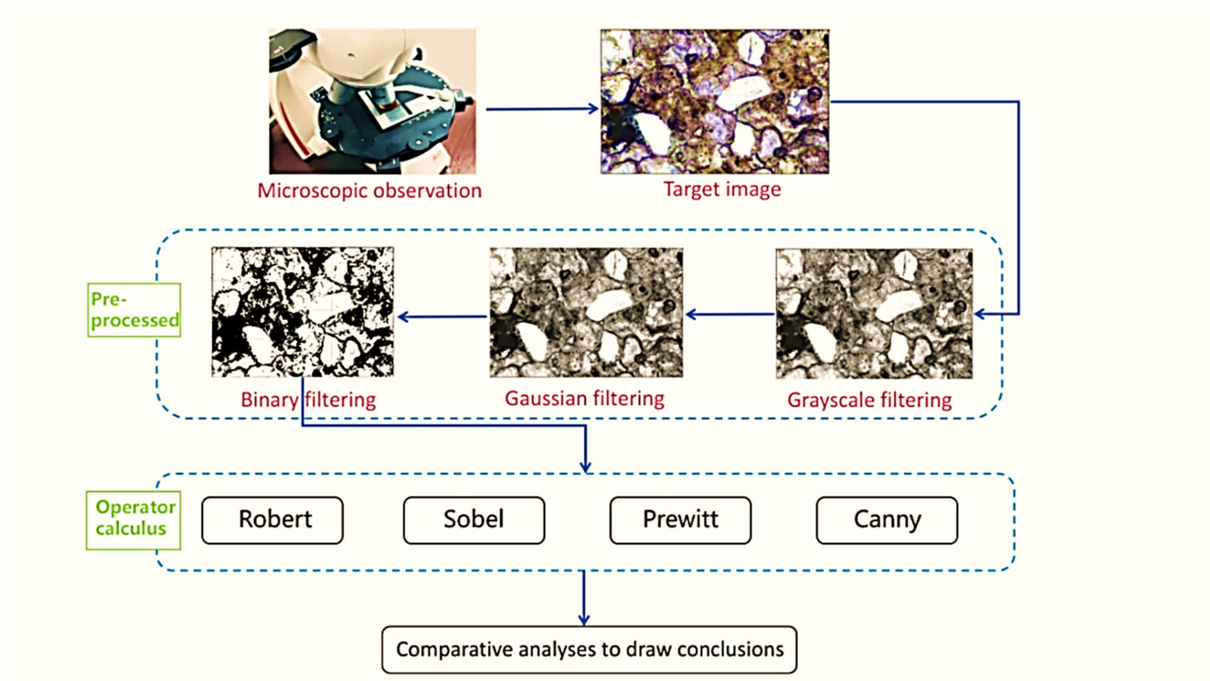

Fig. 4 Microstructure edge extraction scheme.

$$G(x, y) = f(x, y)H(x, y) \tag{7}$$

Where $H(x, y)$ is the Gaussian filter function, $f(x, y)$ is the image data, σ denote the standard deviation.

(II) Pixel gradients and directions are calculated using first-order differential operators.

The gradient magnitude as well as the direction angle of $G(x, y)$ is calculated by the following equation:

$$\varphi(x, y) = \sqrt{(G_x)^2 + (G_y)^2} \tag{8}$$

$$\theta_\varphi = arctan(\frac{G_x}{G_y}) \tag{9}$$

(III) Suppression of non-maximum gradients is applied. Only the point with the largest local gradient is kept while the others are set to zero to obtain edges.

(IV) The double threshold algorithm is used to determine the edge points. Setting a high threshold filters out false edges in the target contour, while a low threshold helps connect broken edges, achieving accuracy tuning.

(V) Isolated weak edge suppression.

2.3. MICROSTRUCTURE EDGE EXTRACTION RESULTS

After acquiring the image of the red-bed soft rocks by polarized light microscope, the microstructure edge extraction scheme is shown in Figure 4.

To enhance image contrast, the microscope-scanned images of the red-bed soft rocks were pre-processed. The pre-processing includes the following steps: Firstly, grey scale processing is applied to the target image to significantly increase image contrast. Gaussian filtering is used to effectively suppress noise, sharpen particle boundaries, and smooth the image while blurring it to a lesser extent than mean filtering. Binarization converts grayscale pixel values in the image to just two states: 0 and 255, resulting in an image composed only of black and white to highlight the boundaries of transparent particles (Cheng and Ding, 2019; Liu and Liu, 2013; Vincent, 1986).

The image of the thin sections of rock shown in Figure 2 under microscope scanning is shown in Figure 5(a). After preprocessing, a binary image is obtained, as shown in Figure 5(b). It should be noted that the numbers in the figure represent pixel coordinates, which are used to locate and mark feature points or regions in the image. Pixel coordinates are commonly used for image analysis and feature extraction. The processed image is then subjected to four commonly used edge detection operator methods to detect the image edges. It can be seen from Figure 5 that the edges detected by the Roberts operator show a large amount of noise, although it can detect the approximate outline. Notably, not many continuous edges are visible, indicating a significant loss of edge information. The principle explains that while the local difference method can provide localized advantages with high accuracy, it suffers from more information loss, which prevents the Roberts operator from obtaining the complete boundary contour. The Sobel and Prewitt operators excel at preserving particle boundary information during differential operations after weighted filtering, making more particle boundaries identifiable. Nonetheless, the gradient operator still faces a severe edge missing

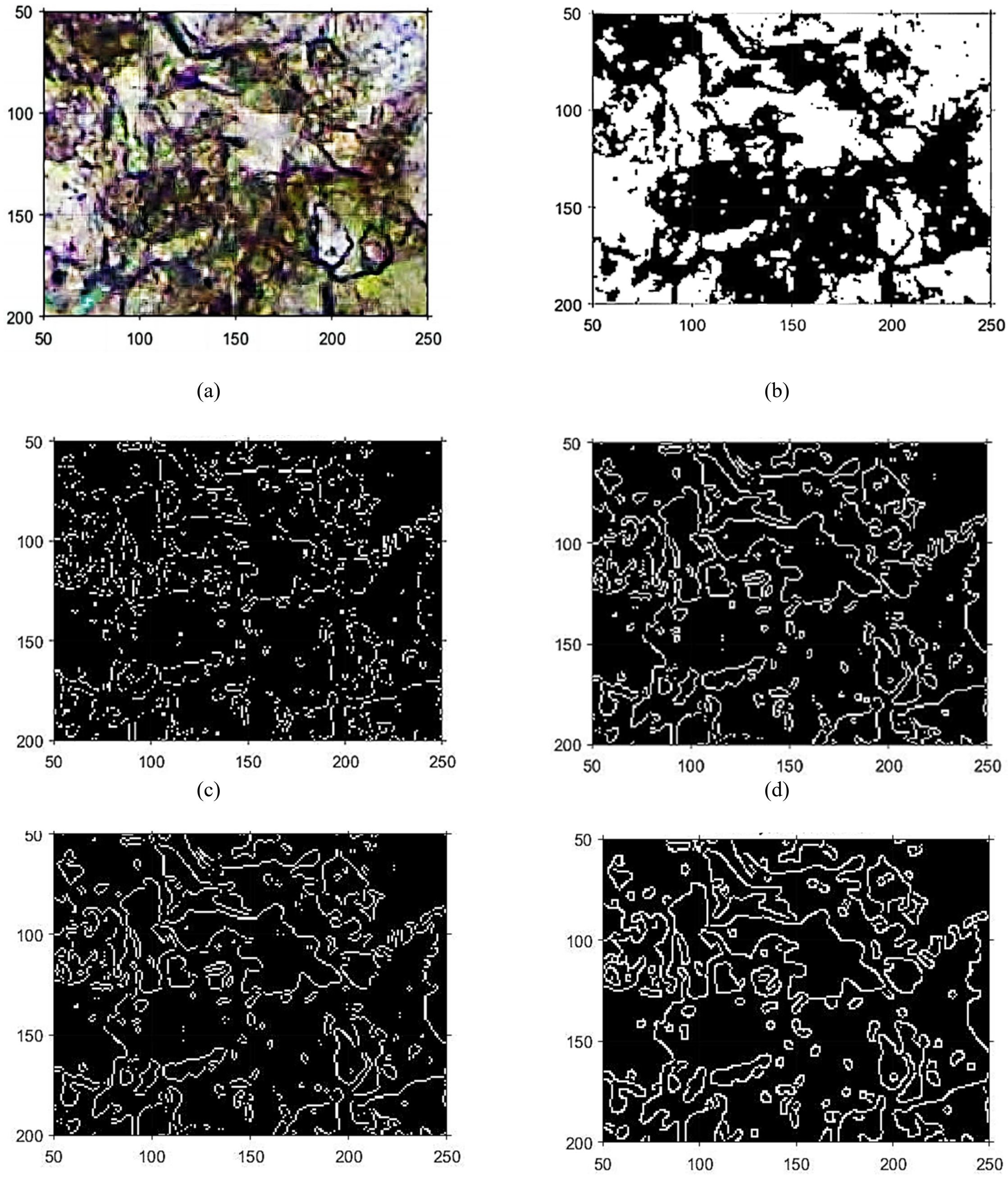

Fig. 5 Results of edge structure extraction from the images of rock microstructure. (a) Original image. (b) Binary image. (c) Robert operator edge detection. (d) Sobel operator edge detection. (e) Prewitt operator edge detection. (f) Canny operator edge detection.

problem, and the differential operation amplifies unremoved noise, introducing significant noise into the results. The Canny operator effectively eliminates some pseudo-edges, thereby maximizing the retention of the particle structure and yielding a clearer structure of the red-bed soft rock. Consequently, the results extracted using the Canny operator method prove more effective in identifying rock particles compared to the other three detection methods.

From the original image and the results of edge extraction by the operator method, it is evident that the image recognition method can effectively extract the edges of rock microstructures while preserving more image details. In the image of red-bed rocks processed with the Canny operator, the outline of each particle is distinct, the deformation is small, and the outline is consistent with that in the original microscopic photograph. This well reproduces the original appearance of the particles and cements and greatly facilitates the quantitative characterization of the microstructure in red-bed rocks.

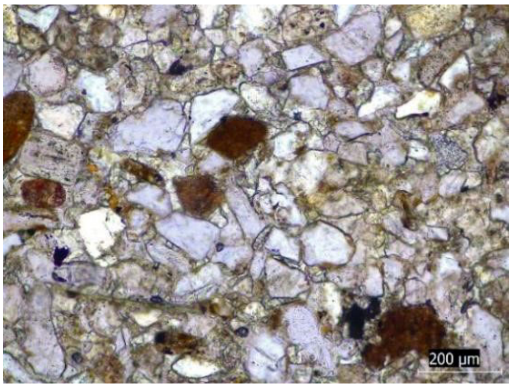

(a)

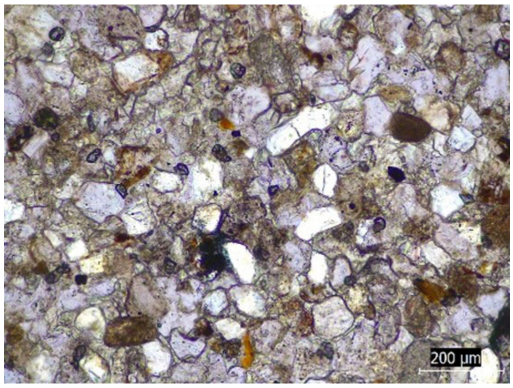

(b)

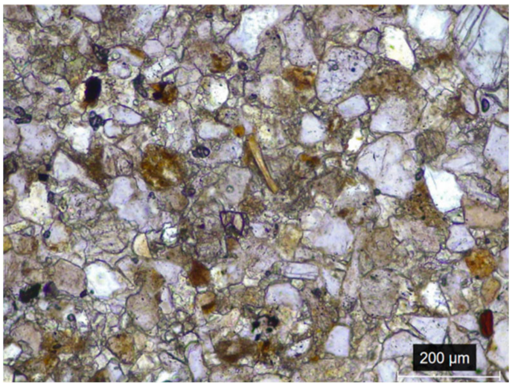

(c)

Fig. 6 Microstructure photographed by polarized light microscope. (a) Sample 1. (b) Sample 2. (c) Sample 3.

3. IMAGE EVALUATION OF MICROSTRUCTURE

Particle size analysis is an essential aspect of rock mechanics research. One objective of particle size analysis is to obtain the particle size distribution. Particle information on rocks is important for understanding the microscopic deformation characteristics of rocks. In this section, the heterogeneity index, calculated from the difference in particle size, is used to quantitatively assess the degree of heterogeneity in the microstructure of red-bed soft rocks

3.1. PARTICLE SIZE ANALYSIS STATISTICS

To evaluate the overall microstructure of rocks and avoid errors in the evaluation results due to the heterogeneity of the same rock, we selected multiple sections from different regions of the same rock sample for polarized light microscopy observations. Specifically, three sections, labeled Sample 1, 2, and 3, were chosen to ensure a more representative analysis of the microstructure. Figure 6 shows the microstructure of red-bed soft rocks obtained from these sections.

The magnification of the picture in Figure 6 is 200 times. It can be seen from the figure that the particles of the red-bed soft rocks are loosely distributed and discrete. Due to the pressure during rock formation, there are adhesions between the mineral particles, causing them to be cemented together.

To further understand the mineralogical composition of red-bed rocks, X-ray diffraction techniques were used for detailed analysis. The results (Fig. 7) show that the main minerals of the red-bed soft rocks are dominated by quartz and calcite, with a small amount of feldspar.

A polarized light microscope was used to obtain images of the particle structure of the red-bed soft rocks. A grain size statistics software, Nano Measurer, was utilized to acquire the grain size of irregular, non-spherical particles from the rock microstructure images obtained by the polarized light microscope (Fig. 8). This program can achieve automatic capture of particle information in rock slicing. Once the particle information was obtained, the average particle size was calculated using the horizontal and vertical Feret diameters of the particles, referencing the method of Liu et al. (2022). Generally speaking, the horizontal and vertical Feret diameters refer to the maximum horizontal and vertical cut-line distances of the particles. The average particle size of irregular particles can be calculated by calculating the average value of the horizontal and vertical Feret diameters of the particles.

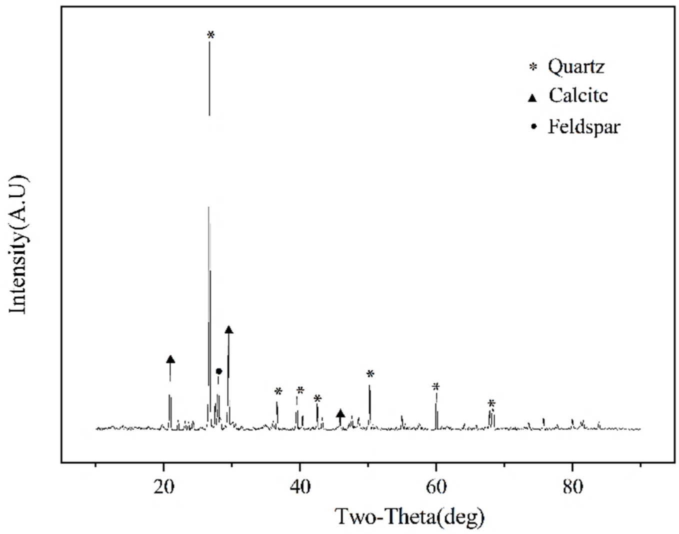

Fig. 7 X-ray diffraction results.

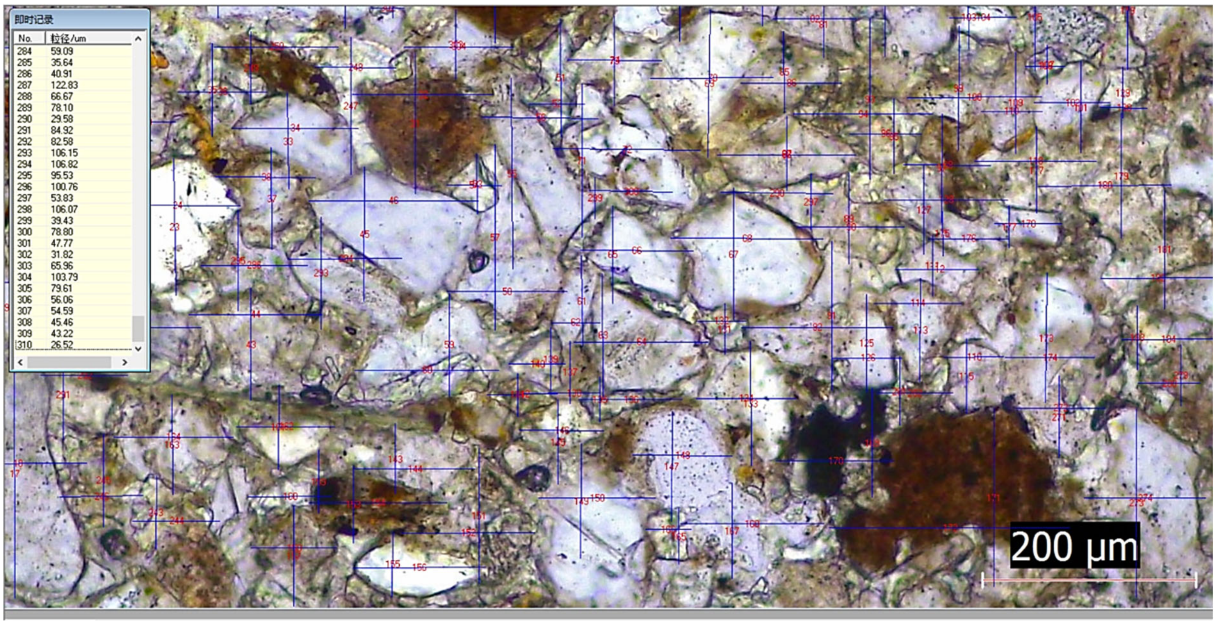

Fig. 8 The horizontal and vertical Feret diameters of the particles

It should be noted that the method above takes incomplete particles at the edges into account when calculating the average Feret diameter. The mean particle diameter statistics were performed for the above three samples, and their particle size distribution is shown in Figure 9. Sample 1, has a maximum particle diameter of 197.42 µm, a minimum particle diameter of 34.87 µm, and an average particle diameter of 90.29 µm. The maximum particle diameter of Sample 2 is 145.37 µm, the minimum particle diameter is 34.87 µm, and the average particle diameter is 82.10 µm. The maximum particle diameter of Sample 3 is 199.70 µm, the minimum particle diameter is 32.85 µm, and the average particle diameter is 88.08µm. From Figure 9, it can be seen that the particle size distribution is relatively uniform and generally follows a normal distribution.

Particle sizes are usually classified as nanoparticles (1-100 nm), submicron particles (0.1-1 µm), micro powder (1-100 µm), fine powder (100-1000 µm), and coarse particles (>1 mm). According to the above particle size distribution statistics, the particle size of red-bed soft rocks is generally distributed in the interval of 47-132 µm, thus falling into the category of micro powder and fine powder. Therefore, red-bed soft rocks often collapse due to the weakening of their structure caused by particle accumulation.

3.2. QUANTITATIVE EVALUATION OF HETEROGENEITY

Differences in particle size are an essential factor in the geometric heterogeneity of rocks (Peng et al., 2019). Differences in particle size in the same rock can lead to heterogeneous local deformation, resulting in

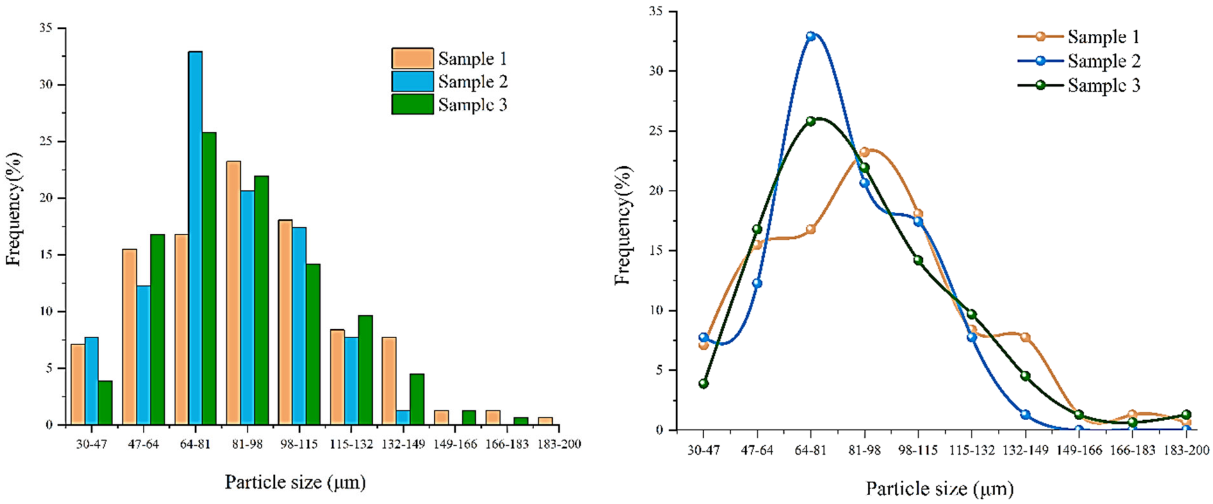

Fig. 9 Particle size distribution map of red-bed soft rock under a polarized light microscope.

Table 1 Calculation table of heterogeneity index.

Sample	Sample 1	Sample 2	Sample 3
H	0.6001	0.4503	0.5671

different failure processes (Hu et al., 2008). Therefore, the heterogeneity caused by the difference in particle size needs to be considered when studying rock's strength and damage deformation mechanisms.

The heterogeneity index proposed by (Liu et al., 2018) remains effective even when there are significant variations in mineral grain sizes and the average grain sizes of different minerals are similar. By comprehensively considering the minimum, average, and maximum grain sizes of each mineral to estimate grain size differences, it significantly enhances its representativeness in measuring microstructural heterogeneity. The equation of the heterogeneity index is as follows.

$$H=\frac{1}{3m}\sum_{i=1}^{m}\sum_{k=1}^{3}\left|\frac{d_{ik}}{d}-1\right| \tag{10}$$

In the equation, d is the model average crystal particle size, m is the number of minerals contained in the rock sample, H is the heterogeneity index, d_{i1}, d_{i2}, and d_{i3} are the minimum particle size, the average particle size, and the maximum particle size of the ith mineral particle respectively.

Calculating the heterogeneity index of a rock using the formula above requires the maximum and minimum particle sizes of each mineral for the average value. In most cases, such detailed mineral information is difficult to obtain. Suppose we consider a rock as a conglomeration of many mineral particles. Therefore, the above equation can be simplified by taking m=1.

$$H=\frac{1}{3}\sum_{k=1}^{3}\left|\frac{d_{k}}{d}-1\right| \tag{11}$$

To quantitatively evaluate the degree of heterogeneity of the microstructure of red-bed soft rocks, this study employs the aforementioned method to calculate the heterogeneity index based on particle size differences. The calculation results are shown in Table 1 below.

As shown in Figure 9, Sample 1 exhibits distinct particle sizes with obvious disparities, whereas Sample 2 shows similar particle sizes with minor variations. Consequently, the heterogeneity indices, from highest to lowest, are Sample 1, Sample 3, and Sample 2, aligning with the heterogeneity index calculation results. Therefore, the heterogeneity index calculated by the particle size difference can quantitatively evaluate the heterogeneity degree of the microstructure of red-bed soft rocks.

CONCLUSIONS

Through microscopic observation and microstructure analysis of red-bed soft rocks taken from the Three Gorges reservoir area, the following main conclusions were obtained:

1. The particle structure of the red-bed soft rocks was extracted from their thin section microscopic images using the four edge image detection operator methods. It is shown that the outline of each particle in the image of red-bed rocks processed with the canny operator is clear and less deformed, which is consistent with the outline in

the original microscopic photograph. The edge detection extraction result from the Canny operator well reproduces the original appearance of the particles and cement, which indicates canny operator method is suitable for the extraction of rock particle morphology.

2. A statistical analysis of the particle size of red-bed soft rocks was carried out by defining the particle size representation of irregular shapes. The degree of heterogeneity of the microstructure of the red-bed soft rock was quantified using the index of particle size heterogeneity. The calculated results were compared with the statistical analysis of particle size of red-bed soft rocks in polarized light micrographs. It is shown that the heterogeneity index can well reflect the micro-geometric heterogeneity of microstructure images and provide a method for quantitatively analyzing the microstructure of red-bed soft rocks.

ACKNOWLEDGEMENTS

This research is supported by the National Natural Science Foundation of China (No. 52009024), the State Key Laboratory of Safety and Health for Metal Mines (2023-JSKSSYS-01), the Key Laboratory of Rock Mechanics and Geohazards of Zhejiang Province (No. ZJRMG-2023-03), the Fundamental Research Funds for the Central Universities (Nos. JZ2022HGTB0273 and PA2021KCPY0031)), and innovation and entrepreneurship funds for returnees of Hefei. These supports are gratefully acknowledged.

REFERENCES

Bilen, C., Er, S., Tuğrul, A. and Murat, Y.: 2021, A new approach for the prediction of brittleness index based on chemical properties of basaltic rocks. Acta Geodyn. Geomater.,18, 03. DOI: 10.13168/AGG.2021.0020

Breithaupt, T., Hansen, L.N., Toppaladoddi, S. and Katz, R.F.: 2021, The role of grain-environment heterogeneity in normal grain growth: A stochastic approach. Acta Mater., 209, 116699. DOI: 10.1016/j.actamat.2021.116699

Canny, J.: 1986, A computational aproach to edge detection. IEEE T. Pattern Anal., 6, 679-698. DOI: 10.1109/TPAMI.1986.4767851

Cheng, H.F. and Ding, L.L.: 2019, Research on gray scale processing algorithm of binary image. Comput. Telecommun., 7, 34-37. DOI: 10.15966/j.cnki.dnydx.2019.07.010

Cheng, X.M. and Cui, Z.: 2008, Reconstructed system of CT image based on contour tracking. Int. Symposium on Computer Science and Technology, 1, 235–238. DOI: 10.1109/ISCSCT.2008.84

Ding, W.H, Wu, Y.Q., Pu, Y.S, Cao, G.Z. and Cui, Z.X.: 2003, Measurement of crack width in rock interior based on X-ray CT. J. Rock Mech. Eng., 22, 9, 1421–1425. DOI: 10.3321/j.issn:1000-6915.2003.09.004

Goral, J., Andrew, M., Olson, T. and Deo, M.: 2020, Correlative core-to pore-scale imaging of shales. Mar. Petrol. Geol., 111, 886–904. DOI: 10.1016/j.marpetgeo.2019.08.009

Hofmann, H., Babadagli, T., Yoon, J.S., Zang, A. and Zimmermann, G.: 2015, A grain based modeling study of mineralogical factors affecting strength, elastic behavior and micro fracture development during compression tests in granites. Eng. Fract. Mech., 147, 261–275. DOI: 10.1016/j.engfr acmech.2015.09.008

Hu, X.H, Wilkinson, D.S., Jain, M. and Mishra, R.K.: 2008, Modeling strain localization using a plane stress two-particle model and the influence of grain level matrix inhomogeneity. J. Eng. Mater. Technol., 130, 2, 021002–021010. DOI: 10.1115/1.2840959

Jing, J.F., Liu, S.J., Wang, G., Zhang, W.C. and Sun, C.M.: 2022, Recent advances on image edge detection: A comprehensive review. Neurocomputing, 503, 259–271. DOI: 10.1016/j.neucom.2022.06.083

Kang, M., Xu, Q.G. and Wang, B.S.: 2008, A Roberts' adaptive edge detection method. J. Xi'an Jiaotong Univ., 42, 10, 1240–1244. DOI: 10.3321/j.issn:0253-987X.2008.10.010.

Kazerani, T.: 2013, Effect of micromechanical parameters of microstructure on compressive and tensile failure process of rock. Int. J. Rock Mech. Min. Sci., 64, 6, 44–55. DOI: 10.1016/j.ijrmms.2013.08.016

Knopp, J., Steger, H., Moormann, C. and Philipp, B.: 2022, Influence of weathering on pore size distribution of soft rocks. Geotech. Geol. Eng., 40, 11, 5333–5346. DOI: 10.1007/s10706-022-02217-3

Li, C., Xu, Q., Shi, B. and Gu, Y.F.: 2018, Digital image recognition method of rock particle and pore system and its application. Chin. J. Geotech. Eng., 40, 5, 925–931. DOI: 10.11779/CJGE201805018

Li, Z., Liu, C. and An, M.: 2012, The design of sobel image edge detection based on FPGA. Modern Scientific Instruments, 4, 84–86.

Liu, G., Cai, M. and Huang, M.: 2018, Mechanical properties of brittle rock governed by micro-geometric heterogeneity. Comput. Geotech., 104, 358–372. DOI: 10.1016/j.compgeo.2017.11.013

Liu, G., Cai, M., Yao, H.Y., Rong, G., Zhang, Z.H. and Wang, Y.Q.: 2022, Strength estimation of granular rocks using a microstructure-based empirical model. Eng. Fail. Anal., 142, 106761. DOI: 10.1016/j.engfailanal.2022.106761

Liu, H.Y., Roquete, M., Kou, S.Q. and Lindqvist, P.A.: 2004, Characterization of rock heterogeneity and numerical verification. Eng. Geo., 72, 1-2, 89–119. DOI: 10.1016/j.enggeo.2003.06.004

Liu, X.W. and Liu, C.Y.: 2013, An optional gauss filter image denoising method based on difference image fast fuzzy clustering. Appl. Mech. Mater., 411, 1348–1352. DOI: 10.3321/j.issn:0253-987X.2008.10.010

Miščević, P., Cvitanović, N.Š. and Vlastelica, G.: 2020, Degradation processes in civil engineering slopes in soft rocks. Soft Rock Mechanics and Engineering., 25, 335–371. DOI: 10.1007/978-3-030-29477-9_12

Miščević, P. and Vlastelica, G.: 2011, Durability characterization of marls from the region of Dalmatia, Croatia. Geotech. Geol. Eng., 29, 771–781. DOI: 10.1007/s10706-011-9416-y

Peng, J., Wong, L.N.Y., Liu, G. and Teh, C.I.: 2019, Influence of initial micro-crack damage on strength and micro-cracking behavior of an intrusive crystalline rock. B. Eng. Geol. Environ, 78, 2957–2971. DOI: 10.1007/s10064-018-1317-3
Vincent, J.: 1986, How grey-scale processing improves vision system performance. Proc. SPIE Automatic Optical Inspection, 654, 123–124. DOI: 10.1117/12.938278
Vlastelica, G., Miščević, P., Cvitanović, N. Š.: 2018, Durability of soft rocks in Eocene flysch formation (Dalmatia, Croatia). Eng. Geol., 245, 207–217. DOI: 10.1016/j.enggeo.2018.08.015
Wang, S., Sloan, S., Sheng, D., Yang, S. and Tang, C.: 2014, Numerical study of failure behaviour of pre-cracked rock specimens under conventional triaxial compression. Int. J. Solids Struct., 51, 5, 1132–1148. DOI: 10.1016/j.ijsolstr.2013.12.012
Wang, X. and Cai, M.: 2018, Modeling of brittle rock failure considering inter- and intra-grain contact failures. Comput. Geotech., 101, 224–244. DOI: 10.1016/j.compgeo.2018.04.016
Xie, X., Ge, S.L., Xie, M.Y., Hu, F.P. and Jiang, N.: 2020, An improved industrial sub-pixel edge detection algorithm based on coarse and precise location. J. Amb. Intel. Hum. Comp., 11, 2061–2070. DOI: 10.1007/s12652-019-01232-2
Zhang, S.G., Yun, X., Song, Y., Liu, W.B. and Yang, L.: 2022, Fluid-structure coupling creep characteristics of red-bed soft rock in South China. Water, 14, 24, 4088. DOI: 10.3390/W14244088
Zhao, K., Ma, H.L., Liang, X.P., Li, X.X., Liu, Y.B., Cai, R., Ye, L.L. and Yang, C.H.: 2022, Damage evaluation of rock salt under multilevel cyclic loading with constant stress intervals using AE monitoring and CT scanning. J. Petrol. Sci. Eng., 208, 109517. DOI: 10.1016/j.petrol.2021.109517
Zhao, Z., Shou, Y. and Zhou, X.: 2023, Microscopic cracking behaviors of rocks under uniaxial compression with microscopic multiphase heterogeneity by deep learning. Int. J. Min. Sci. Technol., 33, 4, 411–422. DOI: 10.1016/j.ijmst.2022.12.008
Zhao, Z. and Zhou, X.-P.: 2020, Establishment of numerical cracking constitutive models using 3D reconstruction and X-ray CT images of geomaterials. Int. J. Mech. Sci., 183, 105814. DOI: 10.1016/j.ijmecsci.2020.105814
Zhou, R.G., Yu, H., Cheng, Y. and Li, F.X.: 2019, Quantum image edge extraction based on improved Prewitt operator. Quantum Inf. Process., 18, 1–24. DOI: 10.1007/s11128-019-2376-5